

Structures of lipoyl synthase reveal a compact active site for controlling sequential sulfur insertion reactions

Jenny E. Harmer^{*1}, Martyn J. Hiscox^{*1}, Pedro C. Dinis^{*}, Stephen J. Fox^{*}, Andreas Iliopoulos^{*}, James E. Hussey[†], James Sandy[†], Florian T. van Beek^{*}, Jonathan W. Essex^{*‡} and Peter L. Roach^{*‡2}

^{*}Chemistry, University of Southampton, Highfield, Southampton, SO17 1BJ (UK).

[†]Diamond Light Source, Didcot OX11 0DE (UK).

[‡]Institute for Life Sciences, University of Southampton, Highfield, Southampton, SO17 1BJ (UK).

¹ These authors are joint first authors for this paper.

²Address correspondence to Prof. Peter L. Roach, email: plr2@soton.ac.uk.

Short title: Structure of Lipoyl Synthase

Summary Statement: The biosynthesis of lipoyl cofactors requires two lipoyl synthase mediated sulfur insertions. We report the crystal structures of a lipoyl synthase complexed with *S*-adenosylhomocysteine or 5'-methylthioadenosine. Models based on these structures identify likely substrate binding sites.

Keywords: radical SAM, cofactors, crystal structure, enzyme catalysis, sulfur

Abbreviations used: LipA, lipoyl synthase; BioB, biotin synthase; SAM, *S*-adenosylmethionine; LCD, lipoyl carrier domain; MTA, 5'-methylthioadenosine; RS, radical SAM; ACP, acyl carrier protein; *Ss*LipA, *Sulfolobus solfataricus* LipA; *Te*LipA2 *Thermosynechococcus elongatus* LipA2; *Ec*, *Escherichia coli*; 5'-dA, 5'-deoxyadenosine.

ABSTRACT

Lipoyl cofactors are essential for living organisms and are produced by the insertion of two sulfur atoms into the relatively unreactive C-H bonds of an octanoyl substrate. This reaction requires lipoyl synthase, a member of the radical SAM enzyme superfamily. Herein we present crystal structures of lipoyl synthase with two [4Fe-4S] clusters bound at opposite ends of the TIM barrel, the usual fold of the radical SAM superfamily. The cluster required for reductive SAM cleavage conserves the features of the radical SAM superfamily, but the auxiliary cluster is bound by a CX₄CX₅C motif unique to lipoyl synthase. The fourth ligand to the auxiliary cluster is an extremely unusual serine residue. Site directed mutants show this conserved serine ligand is essential for the sulfur insertion steps. One crystallized LipA complex contains MTA, a breakdown product of SAM, bound in the likely SAM binding site. Modelling has identified an 18 Å deep channel, well-proportioned to accommodate an octanoyl substrate. These results suggest the auxiliary cluster is the likely sulfur donor, but access to a sulfide ion for the second sulfur insertion reaction requires the loss of an iron atom from the auxiliary cluster, which the serine ligand may enabled.

INTRODUCTION

Lipoyl cofactors are essential for living organisms as they participate in the reactions catalyzed by the 2-oxoacid dehydrogenase (OADH) complexes and the glycine cleavage system [1]. Within each of these multi-component complexes, a specific subunit termed the lipoyl carrier domain (LCD) is functionalized by the attachment of lipoic acid to yield a lipoyl domain. The covalent attachment is formed by an amide bond between the lipoyl carbonyl group and the N^ε of a conserved lysine residue in the LCD of an OADH complex or the H protein of the glycine cleavage system. In *E. coli*, lipoyl groups can be incorporated by at least two routes (Figure 1). Scavenged lipoic acid can be utilized by ATP dependent activation and attachment via an amide bond to the lysine residue of the LCD in a reaction catalyzed by the LplA [2]. Alternatively, *de novo* lipoyl cofactor biosynthesis proceeds initially by octanoylation of the LCD lysine residue [3]. This can occur through LplA catalyzed activation of octanoic acid and octanoylation of the LCD [4], or through the action of an octanoyltransferase, LipB, which catalyzes the transfer of an octanoyl group from octanoyl-ACP to the lysine residue of the LCD [5]. Variations in the transferase and/or ligase enzymes required for *de novo* lipoyl cofactor biosynthesis have been reported in other microbes, but all proceed via octanoylated LCDs [6-8]. Assembly of the octanoyl LCD is followed by insertion of sulfur atoms at C6 and C8 of the octanoyl chain [3]. The sulfur insertion reaction requires lipoyl synthase (LipA), a member of the radical SAM (RS) superfamily [3, 9].

The double sulfur insertion reaction that completes the lipoyl cofactor is regiospecific for C8 and stereospecific with inversion at C6 [10, 11]. The two sulfur atoms are inserted into the relatively unreactive C-H bonds of an octanoyl substrate and reactions introducing functionality at such relatively inert sites are often termed ‘chemically challenging’ [12]. Most members of the RS family, including LipA, reduce SAM to yield the 5'-deoxyadenosyl radical [13]. This intermediate is a highly reactive primary radical capable of abstracting hydrogen atoms from unactivated carbon centers [12]. Consistent with this mode of action and the requirement to break two C-H bonds, the formation of lipoyl groups requires at least two equivalents of SAM [9]. Mutagenesis has identified the presence of two [4Fe-4S] clusters in LipA, each ligated by three cysteine residues [14]. One cluster, [4Fe-4S]_{RS}, is bound by a triad of conserved cysteine residues constituting the CX₃CX₂C motif characteristic of RS enzymes [15] and functions as the reductant in the SAM cleavage reaction. The other cluster, termed the auxiliary cluster ([4Fe-4S]_{Aux}) herein, is bound by a CX₄CX₅C motif that is found exclusively in LipA, close to the N-terminus of the sequence [14]. The function of the auxiliary cluster has not been fully elucidated, but studies with ³⁴S labeled LipA suggest both of the sulfur atoms are transferred from a single LipA molecule [16], which may indicate the auxiliary cluster is functioning as the sulfur donor. The high degree of sequence similarity between biotin synthase and lipoyl synthase [15] which are both required for transformations resulting in sulfur insertion [17] suggests they may function by related mechanisms and kinetic [18], structural [19] and spectroscopic data [20, 21] indicate that the auxiliary [2Fe-2S] cluster of BioB functions is the sulfur donor for biotin formation. A further subgroup of the RS superfamily, the methylthiotransferases, catalyze the insertion of thiomethyl groups into C-H bonds of proteins [22, 23] and nucleic acids [24-26], but these enzymes can use exogenously added sulfide as a sulfur source [27].

N^ε-octanoyl lysine containing peptides have been used as model substrates for SsLipA to yield lipoyl peptides as products [28]. In addition, quenching of an activity assay with acid at an early time point led to the release of a 6-thiooctanoyl peptide, proposed as a monothiolated intermediate on the reaction pathway to the lipoyl product [29]. Recently, evidence for the

catalytic and kinetically competent enzyme-substrate cross-linked intermediate of lipoyl synthase has been reported [30]. The cross-link is proposed to result from a bond between the octanoyl C6 and the presumed sulfur donor, the auxiliary cluster, which is sacrificed during turnover.

In the present study, we have used structural, modeling and biochemical methods to investigate the structure and function of lipoyl synthase. We describe the crystal structures of a lipoyl synthase from *Thermosynechococcus elongatus* at 1.6 Å resolution, including two iron sulfur clusters. In addition to the three cysteine residue ligands, the auxiliary cluster is bound by a highly unusual serine residue and site directed mutagenesis suggests this serine residue is essential for lipoyl group formation, but not required for reductive cleavage of SAM. The active site of one structure contains MTA, a breakdown product of SAM, which is likely located in the SAM binding site. These structures have allowed us to develop a model of substrate binding, including docking of SAM and an octanoyl substrate. Based on these structures, the nearest sulfide ion of [4Fe-4S]_{Aux} cluster is a good candidate to be the first sulfur atom required for lipoyl cofactor formation. To complete the lipoyl cofactor, a second sulfur atom is required. In accord with biochemical results [30] and the active site steric constraints, loss of an iron atom from the auxiliary cluster is required to allow access to the second equivalent of sulfide to complete the lipoyl cofactor. It is likely that the serine ligand facilitates this loss of iron.

EXPERIMENTAL

Subcloning and Expression of *TeLipA2*

A synthetic codon optimized gene encoding (His)₆ tagged *TeLipA2* with 5'-NcoI and 3'-XhoI restriction sites was supplied by Life Technologies. The *T. elongatus lipA2* was subcloned into the NcoI and XhoI restriction sites of the plasmid pFM024 to yield plasmid pMH003. Plasmid pFM024 is a derivative of the plasmid pMK024 in which the second NcoI site has been removed by mutagenesis [28]. An overnight culture of pMH003 in BL21(DE3) cells was used as a 1% inoculum into 2YT (5 L) and cultured at 37 °C. At an optical density of 0.8 at $\lambda = 600$ nm, the temperature was reduced to 27 °C and expression of LipA induced by the addition of sterile-filtered arabinose solution to a final concentration of 1% (w/v). After four hours, cells were harvested by centrifugation (14,000 g, 4 °C, 20 min). Cell pastes (~30 g/5 L) were stored at -80 °C.

Construction and characterization of *SsLipA* mutants

DNA encoding Ser267Ala and Ser267Cys mutations were synthesized and subcloned into pFM024 by Eurofins (Ebersberg, Germany). The proteins were expressed and purified following the protocol described for the wild type enzyme [28]. The mutants and wild type enzyme were characterized by UV-visible spectroscopy (Supplementary Figure S1) and iron analysis (Supplementary Table S1) [7].

Purification of *TeLipA2* for crystallization studies

Cell paste was transferred to an anaerobic chamber (Belle Technologies, less than 2 ppm O₂) and resuspended in buffer A (3 mL/g) [25 mM HEPES (pH 7.5), 500 mM NaCl, 50 mM imidazole, 10% glycerol (w/v)] supplemented with lysozyme (0.1 mg/mL) and benzonase (20 μ L, 5000 U) and stirred for 1 hour. The cells were disrupted by sonication (4 x 10 minutes, 1 second pulse, 20 W). Cell debris was removed by centrifugation (21,900 g, 4 °C, 30 min) and the supernatant applied to a nickel charged chelating sepharose FF column (GE Healthcare,

Little Chalfont, UK, 40 mL, pre-equilibrated with buffer A). The column was then washed with 5 column volumes of buffer A and protein was eluted with buffer B [25 mM HEPES (pH 7.5), 500 mM NaCl, 250 mM imidazole, 10% glycerol (w/v)]. The fractions containing LipA (as judged by the brown color) were pooled and concentrated using an Amicon stirred ultrafiltration cell to ~20 mL, then the buffer was exchanged using a Superdex 75 gel filtration column (GE Healthcare, Little Chalfont, UK, 50 mL, equilibrated in buffer C [25 mM HEPES (pH 7.5), 100 mM NaCl, 10% glycerol (w/v)] for biochemical studies and buffer E [25 mM HEPES (pH 7.5), 500 mM NaCl, 10% glycerol (w/v), 1 mM DTT] for crystallization studies). The purest fractions as judged by SDS-PAGE were pooled, concentrated, aliquoted for reconstitution and stored at -80 °C until required.

When purifying protein for crystallization studies, the iron sulfur clusters of *TeLipA2* were reconstituted and the protein was further purified by size exclusion chromatography. Under strictly anaerobic conditions, all required solutions were freshly prepared just prior to addition using buffer E. DTT (5 mM) was added to *TeLipA2* and stirred for 90 minutes. FeCl₃ (50 mM stock, added to a final concentration of 5 equivalents with respect to *TeLipA2*) was added drop-wise over 10 minutes and the solution stirred for a further 10 minutes before addition of Na₂S.9H₂O (30 mM stock, stock added to a final concentration of 10 equivalents with respect to *TeLipA2*) over 10 minutes and the solution stirred for a further 90 minutes. The protein was then centrifuged (2,000 g, 30 min) to remove precipitated iron sulfide and concentrated to ~3 mL.

The *TeLipA2* (~3 mL) was then applied to a Superdex 75 gel filtration column (300 mL equilibrated in buffer E). Two distinct colored fractions were resolved on this column, the initial black fraction and a second golden-brown colored fraction. The two species were collected separately and fractions were analyzed by SDS-PAGE. The purest fractions from the golden-brown band were pooled and concentrated. The iron sulfur clusters were then reconstituted again, using a modified method with FeCl₃ (5 equivalents with respect to *TeLipA2*) and Na₂S.9H₂O (5 equivalents with respect to *TeLipA2*). The protein was then concentrated to >1 mM for crystallization.

Synthetic octanoyl peptide substrates and lipoyl peptide products

Peptides containing N^ε-(octanoyl)-L-lysine [Lys(Oct)] or N^ε-(lipoyl)-L-lysine [Lys(Lip)] were synthesized by conventional Fmoc solid phase peptide synthesis (described in detail in the Supplementary Methods Section S1). The peptide sequences were: *TeLipA2* Substrate 1, H-Glu-Ser-Val-Lys(Oct)-Ala-Val-OH; *TeLipA2* Substrate 2, H-Glu-Ser-Asp-Lys(Oct)-Ala-Asp-OH; *SsLipA* Substrate, H-Trp-Glu-Thr-Glu-Lys(Oct)-Ile-OH; and *SsLipA* Product, H-Trp-Glu-Thr-Glu-Lys(Lip)-Ile-OH.

***TeLipA2* Activity Assay**

TeLipA2 was thawed under strictly anaerobic conditions and exchanged into buffer D [10 mM ammonium bicarbonate, pH 7.5] using a PD-10 column (GE Healthcare, Little Chalfont, UK). LipA (150 μM), peptide substrate 1 or 2 (300 μM), SAM (1 mM) and dithionite (1 mM) were mixed in a final volume of 100 μL and incubated at 37 °C. Activity assays were quenched after 90 min by the addition of 50% propan-1-ol (80 μL) and 20% perchloric acid (20 μL). Precipitated protein was removed by centrifugation (16,100 g, 5 minutes). Supernatants (50 μL) were analyzed by LCMS (ThermoFinnigan Surveyor MSQ coupled to a Gilson HPLC system, separation on a Phenomenex Kinetex 2.6 μ C18 100 Å 4.6 x 150 mm column, analysis by scanning a mass to charge ratio range of 700-1000). *SsLipA* activity assays was prepared as described previously [28] and analyzed by LCMS.

Determination of the Crystal Structure of *TeLipA2*

To obtain crystals of *TeLipA2* complexed with SAH, *TeLipA2* (0.5 mM) was mixed with SAH (2 mM) and either peptide 1 (1 mM) or peptide 2 (1 mM), then incubated for 1 hour at 20 °C. Crystals were grown using the hanging-drop vapor diffusion method in a drop containing a 1:1 ratio of protein to mother liquor, equilibrating over the precipitant solution of 100 mM bicine pH 8.5, 15% PEG 20,000, 3% dextran sulfate sodium salt. Crystals appeared after one day of equilibration and reached a final size of 300 x 75 x 75 μm in two days. Crystals were flash frozen in liquid nitrogen. Single-wavelength anomalous diffraction and native data sets were collected at Diamond Light Source beamline I02 at a temperature of 100 K at wavelengths of 1.7372 and 0.9795 Å respectively. The structure was phased and solved using Phenix [31], followed by model building and refinement using Coot [32]. The Ramachandran statistics calculated for the structure gave 0% outliers and 98.6% favored side chains. Crystals of *TeLipA2* in complex with DTT and MTA were obtained by a similar procedure, except that the SAH was replaced with SAM (20 mM). The structure was solved using the *TeLipA2*:SAH model for molecular replacement in Phenix [31], followed by model building and refinement using Coot [32]. The Ramachandran statistics calculated for the structure gave 1.1% outliers and 95.2% favored side chains.

Modelling substrate binding with *TeLipA2*

Hydrogen atoms were added to the protein structure using Protonate3D [33] in the MOE program [34]. In the crystal structure, the protein is complexed with DTT and 5'-MTA. The DTT is bound to the unique iron of the [4Fe-4S]_{RS} in the position that the methionine of SAM would occupy. DTT was removed from the structure, which was then superimposed with that of HydE (PDB code: 3IIZ). Using the alignment of SAM with MTA and the [4Fe-4S]_{RS}, SAM was modelled into the *TeLipA2* binding pocket with the correct pose and was relaxed using the MMFF94 force field [35]. The octanoyl ligand binding site was initially identified using AutoDock [36], taking the pose with the best agreement to the pocket which was identified using the program HOLLOW [37]. The octanoyl substrate used for modelling was N^ε-octanoyl lysine methylamide. The ligands and the pocket residues were then relaxed using the MMFF94 force field.

RESULTS

Protein Production, Crystallization and Structure Determination

The genome of the thermophilic cyanobacterium *Thermosynechococcus elongatus* BP-1 encodes two lipoyl synthases. One of these, termed *TeLipA2* (Uniprot accession code Q8DLC2), was co-expressed in BL21(DE3) with proteins of the *E. coli* ISC operon [38] and purified from cleared lysates by Ni-affinity chromatography, followed by size exclusion chromatography on Superdex S-75. The purification yielded 90 mg of protein from 35 g of cell paste. Iron sulfur clusters were chemically reconstituted and the efficiency of reconstitution was determined by measuring the UV-visible spectrum, which gave an OD₄₁₀/OD₂₈₀ of ~0.5 (Supplementary Figure S1B). The activity of *TeLipA2* confirmed by LCMS analysis (Supplementary Figure S2).

Crystallization screening by the sitting drop vapor diffusion method yielded small crystals after one day and the size was optimized in subsequent hanging drop experiments. The structure was solved in the space group C222₁ in a single wavelength anomalous dispersion (SAD) experiment. Two complexes of *TeLipA2* were crystallized, but despite including octanoyl peptides corresponding in sequence to LCDs, co-crystals with octanoyl peptides

were not obtained. When crystallized from drops containing *S*-adenosylhomocysteine (SAH), only electron density corresponding to the homocysteine portion of SAH and the 5'-carbon of the adenosyl group can be observed and we term this the *TeLipA2*:SAH complex (Figure 2A). From drops containing SAM, the crystal structure of *TeLipA2* with the SAM breakdown product MTA was solved, termed the *TeLipA2*:MTA complex (Supplementary Figure 2B). The *TeLipA2*:SAH structure contains a single protein monomer in the asymmetric unit, covering from Arg5 to the C-terminal residue, Glu288 with no gaps.

Structure of *TeLipA2*

The most common overall topology observed for the RS superfamily is a partial ($\beta_6\alpha_6$) TIM barrel [39], but the structure of *TeLipA2* complexed with SAH (Figure 2B) includes an extra strand of β -sheet to give a partial ($\beta_7\alpha_6$) TIM barrel (Figure 2C). Two [4Fe-4S] clusters are located within the TIM barrel and are bound by cysteine triads [14]. Comparison with other RS enzymes [40] indicates the cluster responsible for the reductive cleavage of SAM, [4Fe-4S]_{RS}, is bound to cysteines 63, 67 and 70 on the loop between strand β -1 and helix α -1. The auxiliary cluster, [4Fe-4S]_{Aux} is bound by three residues from the N-terminal extension, cysteines 37, 42 and 48. A residue from the C-terminal extension of *TeLipA2*, serine 283, provides the final ligand to the auxiliary cluster. The first helix and loop of the N-terminal extension (residues 5-21) adopt an extended conformation in the SAH complex (Figure 2B) but in the MTA complex, this region was partially disordered (Figure 2A).

Comparison of the overall fold of *TeLipA2* with other RS enzymes using the Dali server [41] showed most similarity to pyruvate formate lyase activating enzyme (Pfl-Ae, PDB 3C8F), HydE (PDB 3IIX) and biotin synthase (PDB 1R30). An overlay of *TeLipA2*, BioB [19], HydE [42] and Pfl-Ae [43] shows the MTA adenine base and ribose ring approximately overlay the positions expected for adenosyl moiety of SAM (Supplementary Figure S3). DTT is bound to directly to the unique iron of the [4Fe-4S]_{RS} through one of the thiols (Figure 2A) and therefore occupies the ligand site typically occupied by the methionine moiety of SAM. As a result, the 'GGE' sequence motif, which in other RS enzymes forms hydrogen bonds to the SAM amino group [19, 40], has no H-bonding partner in the *TeLipA2*:MTA structure. Two motifs shared by RS enzymes and previously described as recognizing SAM [40, 44] form interactions with the MTA (Figure 3C). Firstly, the 'ribose motif' includes residues Asn169 and Glu171 which are positioned to form hydrogen bonds to the 2' and 3' hydroxyl groups of the ribose ring. Secondly, the RS enzyme 'GxIxGxxE' motif, corresponding to the *TeLipA2* sequence G(208)LMLGLGE(215) and the thioether of Met210 packs against the adenine pyrimidine ring. These interactions confirm the adenine and ribose of MTA are positioned in the anticipated binding site for the SAM adenosyl moiety. Finally, the guanidino group of Arg281 is positioned to make a π -cation interaction with the other face of the aromatic adenine base (Figure 3C). This is a well characterized mode of interaction for the recognition of adenosyl ligands [45], but has not previously been observed for the RS enzyme superfamily.

The [4Fe-4S]_{Aux} cluster is enveloped in the N-terminal extension (Figure 2A, helices α -1, α -2 and α -3). This cluster is held in place by three conserved cysteine residues [14] and an unanticipated ligand from close to the C-terminus, Ser283. Serine is previously unreported as a natural ligand for [4Fe-4S] clusters, although this residue has been introduced as a cluster ligand by site directed mutagenesis [46-51]. In the *TeLipA2*:SAH complex structure, the Ser283 alkoxy oxygen atom lies in close proximity to an additional metal atom, which because of its abundance in the crystallization medium (initially approximately 160 mM), has been modeled as a sodium ion (Na-O distance 2.5 Å, Figure 3B).

The auxiliary cluster has tentatively been proposed to act as the sulfur donor in the reaction [30, 52]. Extending between the adenosyl moiety and auxiliary cluster is a 14 Å deep channel that is well-proportioned to accommodate the substrate N^ε-octanoyl lysine residue in an extended conformation. This channel runs from the entrance, bordered by Gly39 and the guanidino group of Arg281, between the auxiliary cluster and the adenosyl moiety of MTA to the far end near Leu138 and Val102 (Figure 3C). Arg281, which interacts with the adenosyl nucleoside also defines part of the channel, as does the proximal μ_3 -sulfide of the auxiliary cluster. In the *TeLipA2*:SAH structure, the sodium ion close to the auxiliary cluster (Figure 2B) partly occludes this channel and is likely expelled upon octanoyl substrate binding. When considering the mechanism of C-S bond formation, the distance between the sites of radical generation and the sulfur donor is crucial: the distance between the unique iron of the RS cluster and the nearest μ_3 -sulfide ion of cluster II is 12.7 Å. A second channel, bordered by residues Cys48, Thr53, Tyr100, Val102, Tyr284, His 285 and Ala286 provides a connection from the auxiliary cluster to the exterior of the protein. We term this the C-channel to reflect its proximity to the protein C-terminal loop.

Modelling Substrate Binding

The *TeLipA2*:MTA:DTT structure was superimposed with that of HydE complexed with SAM (PDB code:3IIZ) and guided by these structures, SAM was modelled manually into the *TeLipA2* in the correct pose. The resultant complex of SAM and *TeLipA2* was energy minimized to establish the hydrogen bonding network. In a second step, N^ε-octanoyl lysine methylamide was manually docked into the channel that runs between the SAM and the auxiliary cluster, which required the displacement of Arg283. The *TeLipA2*:SAM:octanoyl substrate ternary complex was then energy minimized and the resultant model shows the cavity between the clusters is sufficiently long to accommodate the octanoyl substrate (Figure 4A). A space-filling model shows the octanoyl substrate sandwiched between the adenosyl moiety of SAM and the auxiliary cluster, approaching van der Waals contact with the adenosyl moiety of SAM (Figure 4B). The floor of the hydrophobic cavity binding the octanoyl substrate is formed by three strands of the β -sheet, using Thr55 and Leu57 from strand β -1, Val102 and Thr104 from strand β -2 and Leu138 from strand β -3. Ile36, the β - and γ -CH₂s of Arg281 and the β -CH₂ of Ser282 provide further interactions with the octanoyl substrate.

The octanoyl substrate binding model reveals the key spatial relationships between the substrates and the iron sulfur clusters. The SAM sulfonium sulfur atom is 4.4 Å from the proximal iron atom of the RS cluster, similar to the distances observed in structures of RS enzymes co-crystallized with SAM (3.1-4.0Å) [40]. For the hydrogen abstraction step, the distance from the SAM 5' carbon to the octanoyl chain carbon atoms are 4.4 Å to C6 and 5.2 Å to C8 (Figure 4C). The distance between octanoyl C6, the site of the substrate radical, and the potential sulfur donor, the proximal sulfur atom of the auxiliary cluster, is 6.4 Å. One of the other three sulfur atoms from the auxiliary cluster is proposed to be incorporated as the second atom of the lipoyl product [30, 52], but the distance between these sulfides and the octanoyl C8 are 8.2, 8.4, 10.0 Å. For the C8 centered radical to react with one of these sulfide ions, the observed loss of an iron atom from the auxiliary cluster [30] may provide access, together with a conformational change in the octanoyl substrate. On the opposite side of the auxiliary cluster from the octanoyl substrate binding site is the C-channel that stretches from Ser283 to the surface, a distance of over 11 Å, lying between the C-terminal loop (residues 283-288) and the β -sheet of the TIM barrel (Figure 4D). The presence of at least six water molecules and the side chains of polar residues Glu136, Lys206 and Arg234 indicate the hydrophilic nature of this second channel.

Mutation of the Auxiliary Cluster Serine Ligand

To investigate the functional importance of the serine ligand to the auxiliary cluster, two mutants were prepared: one mutant replacing serine with alanine, abolishing its potential to act as a ligand and a more conservative mutation, converting the serine to a cysteine residue. Previously we have assayed the lipoyl synthase activity using *SsLipA* [28] and in *SsLipA*, the serine ligand to the auxiliary cluster is residue 267. To obtain results comparable with earlier activity assay measurements, mutants of *SsLipA* were prepared: Ser267Ala and Ser267Cys. The *SsLipA* activity assay included an octanoyl peptide substrate and the nucleotidase MTAN which hydrolyzes 5'-dA to adenine, minimizing product inhibition by 5'-dA [53]. The acid quenched assay mixtures were analyzed by LCMS to quantify the lipoyl peptide product (Figure 5). Calibration curves for the products were prepared and a heptanoyl peptide was added to the quenched assay to provide an internal standard of known concentration. Additional assays without MTAN were used to quantify the direct SAM cleavage activity of the mutants. The acid quenched assays were analyzed by HPLC (Figure 5). The wild type enzyme formed $52 \pm 1.2 \mu\text{M}$ of lipoyl peptide, approx. 0.35 mol equivalents relative to *SsLipA*, but both mutants produced no lipoyl product (within the error of the measurement). We do not understand the reason for the sub-stoichiometric turnover of *SsLipA*, but a similar phenomenon has been reported for *EcLipA* with octanoyl H-protein as substrate [30]. This contrasts with the results for SAM turnover, as the wild type enzyme showed significant uncoupled turnover, producing ~ 5 mol equivalents of 5'-dA (relative to *SsLipA*), while the mutants S267A and S267C produced 1.26 and 1.20 equivalents.

DISCUSSION

The overall fold of *TeLipA2* is a partial $\beta_7\alpha_6$ TIM barrel, with an N-terminal extension bearing the auxiliary cluster filling the open side of the barrel (Figure 2). Two substantial channels within the structure have openings at either end of the barrel. One channel runs between the [4Fe-4S] clusters and can accommodate both of the substrates (Figure 4). The second cavity, the C-channel, reaches from the opposite side of the auxiliary cluster to the protein surface (Figure 4A). Most of the structurally characterized members of the RS family accommodate iron sulfur clusters and smaller substrates within the $\frac{3}{4}$ TIM barrel fold, with larger substrates binding to the cavity along the open face of the barrel. In this regard, the substrate binding cavity of *TeLipA2* is typical, with the gap between strands β_1 and β_7 occupied by the auxiliary cluster, completing the substrate binding cavity (Figures 2 and 4). The C-channel is a more unusual feature: in some RS enzymes, the end of the TIM barrel is closed off by close packed hydrophobic residues [40], but the unusually large cavity within HydE has three potential access channels and one of these, E2, correlates with the position of the C-channel of *TeLipA2*.

A proposed mechanism for lipoyl synthase, including the highly unusual suggestion that the auxiliary cluster acts as a sacrificial sulfur donor, has been developed in the light of biochemical and spectroscopic studies [29, 30, 52, 54]. Using a N^ϵ -octanoyl lysinyl peptide as a substrate analogue, a monothiolated species was isolated from activity assays and NMR analysis demonstrated that the sulfur insertion had occurred exclusively at C-6 (and not at C-8) [29]. This result is most simply explained in terms of sequential sulfur insertion reactions, firstly at C6 to form a 6-thiooctanoyl intermediate followed by a second sulfur insertion at C8 to complete the lipoyl cofactor. Recent biochemical experiments have demonstrated that a 6-thiooctanoyl peptide or LCD are chemically and kinetically competent intermediates on the

pathway to lipoyl product formation [30]. This is proposed to occur by abstraction by a 5'-deoxyadenosyl radical of the octanoyl C6 pro-*R* hydrogen atom to form a C6 carbon centered radical (Figure 6, 4) followed by reaction with a μ_3 -sulfide from the auxiliary cluster to yield a 6-thiooctanoyl peptide or protein intermediate cross-linked to the auxiliary cluster (Figure 6, 5). Mössbauer spectroscopy of a sample enriched in the cross-linked 6-thiooctanoyl intermediate has revealed formation of the 6-thiooctanoyl intermediate correlates with the loss of one iron atom from a cluster at this stage, giving a [3Fe-3S-1RS] complex (where 1RS indicates the 6-thiooctanoyl peptide, Figure 6, 6).

Several aspects of our structural results are in accord with this mechanistic proposal. The *TeLipA*:MTA complex indicates the likely binding site for SAM and the remaining volume can accommodate a modelled octanoyl substrate in a predominantly hydrophobic cavity (Figure 4A). This model leaves the octanoyl C6 carbon poised between the radical source, the 5'-C of SAM at 4.4 Å and the proposed sulfur donor, the proximal sulfide ion of the auxiliary cluster at 6.2 Å. These distances allow formation of an octanoyl C6 radical and makes quenching this carbon centered radical by reaction with auxiliary cluster sulfide chemically feasible. Another member of the RS superfamily, biotin synthase, catalyzes a mechanistically related sulfur insertion reaction using an [2Fe-2S] cluster as the sulfur donor [21, 55-58]. In the biotin synthase crystal structure, which includes the proposed sulfur donor [2Fe-2S] cluster and the substrate dethiobiotin [19], the relevant distances (5'-C of SAM to DTB C9 and DTB C9 to the proximal sulfur of the [2Fe-2S] cluster) are approximately comparable at 3.9 and 4.1 Å respectively.

The presence of a serine residue as a naturally occurring ligand for a protein bound [4Fe-4S] cluster has not been previously observed, but a serine for cysteine site directed mutation has often been used to modulate or eliminate cluster activity [46-51]. Examination of the electron density near the auxiliary cluster (Figure 3B) shows clear density for the serine ligand (Ser283) with a short Fe-O bond length (1.8 Å in the MTA complex), which likely reflects deprotonation of the serine ligand. Deprotonation is consistent with the reported pKa of 4.75 for the introduced serine in a *Pyrococcus furiosus* ferredoxin mutant with a serine and three cysteine ligands to the [4Fe-4S] cluster [47]. In the *TeLipA2*:SAH complex structure, the serine oxygen atom lies in close proximity to an additional metal atom, which because of its abundance in the crystallization medium (initially approximately 160 mM), has been modelled as a sodium ion (Na-O distance 2.5 Å, Figure 3B). The presence of the sodium acting as a partial counter-ion to the Ser283 alkoxide causes an increase in the iron to Ser283 oxygen bond length to 2.1 Å.

Both the crystal structures and mutant activity assays point to an important role of Ser283 in the mechanism of LipA. Addition of the octanoyl substrate C6 radical to the auxiliary cluster at the proximal μ_3 sulfide will result in a decreased positive charge on the cluster iron atoms, which in turn may result in protonation and release of the Ser283. The formation of the spectroscopically characterized [3Fe-3S-1RS]¹⁺ cluster (where RS is the 6-thiooctanoyl intermediate) requires expulsion of a partially ligated iron atom, which likely occurs via the C-channel (Figure 6, 3→4). The lack of lipoyl product from the S267A mutant and the more conservative S267C mutant confirms the important role for the serine ligand for the sulfur insertion steps. The wild type and both mutants catalyzed reductive cleavage of SAM indicating that the mutations have not caused gross structural changes, although the reduced extent of uncoupled turnover for the mutants is difficult to interpret.

The mechanism for the formation of the second C-S bond between the octanoyl C8 and the sulfur donor, presumably a second auxiliary cluster sulfide, is more challenging. From the

model of *TeLipA2* with SAM and the octanoyl substrate, the distance between the octanoyl C8 carbon and the distal sulfide ions are 8.0, 8.2 and 10.0 Å respectively and the auxiliary cluster iron atoms sterically block access to these sulfide ions. The loss of iron from LipA observed during the formation of the cross-linked 6-thiooctanoyl intermediate [30] (Figure 6, 4) may allow the octanoyl chain access to a sulfide ion that permits the second sulfur insertion at C8. Spectroscopic studies also indicate that upon formation of the second C-S bond, the remainder of the auxiliary cluster is released into free solution with the lipoyl product (Figure 6, 7) [30].

There are significant parallels between this proposed mechanism for LipA and the mechanism proposed for biotin synthase, including using a sacrificial iron sulfur cluster as the sulfur donor and the presence of an unusual ligand in the donor (LipA, Ser283; BioB, Arg95). In the presence of iron sulfur cluster biosynthetic machinery that can reassemble the [2Fe-2S] cluster after each reaction cycle, catalytic activity of BioB has been demonstrated [59]. It may be that a similar reassembly process is required for the [4Fe-4S] auxiliary cluster of lipoyl synthase, but this remains experimentally untested. The proposed sacrificial role of the auxiliary clusters of BioB and LipA contrasts significantly with the proposed mechanism of the methylthiotransferases MiaB [24, 25] and RimO [22, 23, 26]. The structure of *holo*-RimO [27] includes a pentasulfide (S_5^{2-}) ligand bridging between two [4Fe-4S] clusters separated by only 8 Å. The biochemical and structural data for MiaB led to a proposed mechanism in which an exogenous sulfur donor (such as MeS^-) is activated by binding to the auxiliary cluster at an otherwise free binding site (i.e. without a permanent protein ligand in the resting state) [26]. The multiple turnovers of both RimO and MiaB with CH_3Se^- or CH_3S^- substrates support this hypothesis [27].

CONCLUSION

Structures of *TeLipA2* have shown the spatial relationship between the two [4Fe-4S] clusters present in the active site cavity, the binding of an adenosyl nucleoside between them and the presence of an unprecedented serine residue as a ligand to the auxiliary cluster. Modelling has shown that the active site cavity that can accommodate SAM bound to the RS cluster and octanoyl substrate sandwiched between the SAM and the auxiliary cluster. Mutagenesis has shown this serine ligand is essential for lipoyl product formation. In the context of biochemical and spectroscopic results [29, 30], our results support a radical mediated mechanism of sulfur insertion at C6 and then C8 of the octanoyl chain, a process that leads to degradation of the sulfur donating auxiliary cluster. This aspect of the LipA mechanism resembles that proposed for biotin synthase [19, 21], but differs significantly from the mechanism proposed for the methylthiotransferases RimO and MiaB [27].

AUTHOR CONTRIBUTIONS

Jenny E. Harmer, Martyn J. Hiscox, Pedro C. Dinis, Stephen J. Fox, Jonathan W. Essex and Peter L. Roach conceived and designed experiments; Jenny E. Harmer, Martyn J. Hiscox, Pedro C. Dinis, Stephen J. Fox, Andreas Iliopoulos, James E. Hussey, James Sandy and Florian T. van Beek performed the research; Jonathan W. Essex and Peter L. Roach supervised the research. All authors contributed to the manuscript.

ACKNOWLEDGEMENTS

We thank the staff and scientists at Diamond Light Source for their assistance with data collection and analysis. We thank Stuart C. Findlow for assistance with N.M.R. analysis.

FUNDING

The research was supported by the University of Southampton and by the Biotechnology and Biological Sciences Research Council (studentship to M.J.H. and grant BB/J017302/1 to J.W.E.).

REFERENCES

- 1 Perham, R. N. (2000) Swinging arms and swinging domains in multifunctional enzymes: catalytic machines for multistep reactions. *Annu Rev Biochem.* **69**, 961-1004
- 2 Green, D. E., Morris, T. W., Green, J., Cronan, J. E., Jr. and Guest, J. R. (1995) Purification and properties of the lipoate protein ligase of *Escherichia coli*. *Biochem J.* **309** (Pt 3), 853-862
- 3 Zhao, X., Miller, J. R., Jiang, Y., Marletta, M. A. and Cronan, J. E. (2003) Assembly of the covalent linkage between lipoic acid and its cognate enzymes. *Chem Biol.* **10**, 1293-1302
- 4 Morris, T. W., Reed, K. E. and Cronan, J. E., Jr. (1994) Identification of the gene encoding lipoate-protein ligase A of *Escherichia coli*. Molecular cloning and characterization of the *lplA* gene and gene product. *J Biol Chem.* **269**, 16091-16100
- 5 Jordan, S. W. and Cronan, J. E., Jr. (2003) The *Escherichia coli* *lipB* gene encodes lipoyl (octanoyl)-acyl carrier protein:protein transferase. *J Bacteriol.* **185**, 1582-1589
- 6 Christensen, Q. H., Martin, N., Mansilla, M. C., de Mendoza, D. and Cronan, J. E. (2011) A novel amidotransferase required for lipoic acid cofactor assembly in *Bacillus subtilis*. *Mol Microbiol.* **80**, 350-363
- 7 Christensen, Q. H. and Cronan, J. E. (2010) Lipoic acid synthesis: a new family of octanoyltransferases generally annotated as lipoate protein ligases. *Biochemistry.* **49**, 10024-10036
- 8 Hermes, F. A. and Cronan, J. E. (2013) The role of the *Saccharomyces cerevisiae* lipoate protein ligase homologue, *Lip3*, in lipoic acid synthesis. *Yeast.* **30**, 415-427
- 9 Cicchillo, R. M., Iwig, D. F., Jones, A. D., Nesbitt, N. M., Baleanu-Gogonea, C., Souder, M. G., Tu, L. and Booker, S. J. (2004) Lipoyl synthase requires two equivalents of S-adenosyl-L-methionine to synthesize one equivalent of lipoic acid. *Biochemistry.* **43**, 6378-6386
- 10 White, R. H. (1980) Stable isotope studies on the biosynthesis of lipoic acid in *Escherichia coli*. *Biochemistry.* **19**, 15-19
- 11 Parry, R. J. and Trainor, D. A. (1978) Biosynthesis of Lipoic Acid .2. Stereochemistry of Sulfur Introduction at C-6 of Octanoic-Acid. *Journal of the American Chemical Society.* **100**, 5243-5244
- 12 Booker, S. J. (2009) Anaerobic functionalization of unactivated C-H bonds. *Curr Opin Chem Biol.* **13**, 58-73
- 13 Hiscox, M. J., Driesener, R. C. and Roach, P. L. (2012) Enzyme catalyzed formation of radicals from S-adenosylmethionine and inhibition of enzyme activity by the cleavage products. *Biochim Biophys Acta.* **1824**, 1165-1177
- 14 Cicchillo, R. M., Lee, K. H., Baleanu-Gogonea, C., Nesbitt, N. M., Krebs, C. and Booker, S. J. (2004) *Escherichia coli* lipoyl synthase binds two distinct [4Fe-4S] clusters per polypeptide. *Biochemistry.* **43**, 11770-11781
- 15 Sofia, H. J., Chen, G., Hetzler, B. G., Reyes-Spindola, J. F. and Miller, N. E. (2001) Radical SAM, a novel protein superfamily linking unresolved steps in familiar biosynthetic pathways with radical mechanisms: functional characterization using new analysis and information visualization methods. *Nucleic Acids Res.* **29**, 1097-1106

- 16 Cicchillo, R. M. and Booker, S. J. (2005) Mechanistic investigations of lipoic acid biosynthesis in *Escherichia coli*: both sulfur atoms in lipoic acid are contributed by the same lipoyl synthase polypeptide. *J Am Chem Soc.* **127**, 2860-2861
- 17 Fugate, C. J. and Jarrett, J. T. (2012) Biotin synthase: Insights into radical-mediated carbon-sulfur bond formation. *Bba-Proteins Proteom.* **1824**, 1213-1222
- 18 Taylor, A. M., Farrar, C. E. and Jarrett, J. T. (2008) 9-Mercaptodethiobiotin is formed as a competent catalytic intermediate by *Escherichia coli* biotin synthase. *Biochemistry.* **47**, 9309-9317
- 19 Berkovitch, F., Nicolet, Y., Wan, J. T., Jarrett, J. T. and Drennan, C. L. (2004) Crystal structure of biotin synthase, an S-adenosylmethionine-dependent radical enzyme. *Science.* **303**, 76-79
- 20 Fugate, C. J., Stich, T. A., Kim, E. G., Myers, W. K., Britt, R. D. and Jarrett, J. T. (2012) 9-Mercaptodethiobiotin is generated as a ligand to the [2Fe-2S]⁺ cluster during the reaction catalyzed by biotin synthase from *Escherichia coli*. *J Am Chem Soc.* **134**, 9042-9045
- 21 Ugulava, N. B., Sacanell, C. J. and Jarrett, J. T. (2001) Spectroscopic changes during a single turnover of biotin synthase: destruction of a [2Fe-2S] cluster accompanies sulfur insertion. *Biochemistry.* **40**, 8352-8358
- 22 Anton, B. P., Saleh, L., Benner, J. S., Raleigh, E. A., Kasif, S. and Roberts, R. J. (2008) RimO, a MiaB-like enzyme, methylthiolates the universally conserved Asp88 residue of ribosomal protein S12 in *Escherichia coli*. *Proc Natl Acad Sci U S A.* **105**, 1826-1831
- 23 Arragain, S., Garcia-Serres, R., Blondin, G., Douki, T., Clemancey, M., Latour, J. M., Forouhar, F., Neely, H., Montelione, G. T., Hunt, J. F., Mulliez, E., Fontecave, M. and Atta, M. (2010) Post-translational modification of ribosomal proteins: structural and functional characterization of RimO from *Thermotoga maritima*, a radical S-adenosylmethionine methylthiotransferase. *J Biol Chem.* **285**, 5792-5801
- 24 Pierrel, F., Bjork, G. R., Fontecave, M. and Atta, M. (2002) Enzymatic modification of tRNAs: MiaB is an iron-sulfur protein. *J Biol Chem.* **277**, 13367-13370
- 25 Pierrel, F., Douki, T., Fontecave, M. and Atta, M. (2004) MiaB protein is a bifunctional radical-S-adenosylmethionine enzyme involved in thiolation and methylation of tRNA. *J Biol Chem.* **279**, 47555-47563
- 26 Landgraf, B. J., Arcinas, A. J., Lee, K. H. and Booker, S. J. (2013) Identification of an intermediate methyl carrier in the radical S-adenosylmethionine methylthiotransferases RimO and MiaB. *J Am Chem Soc.* **135**, 15404-15416
- 27 Forouhar, F., Arragain, S., Atta, M., Gambarelli, S., Mouesca, J. M., Hussain, M., Xiao, R., Kieffer-Jaquinod, S., Seetharaman, J., Acton, T. B., Montelione, G. T., Mulliez, E., Hunt, J. F. and Fontecave, M. (2013) Two Fe-S clusters catalyze sulfur insertion by radical-SAM methylthiotransferases. *Nat Chem Biol.* **9**, 333-338
- 28 Bryant, P., Kriek, M., Wood, R. J. and Roach, P. L. (2006) The activity of a thermostable lipoyl synthase from *Sulfolobus solfataricus* with a synthetic octanoyl substrate. *Anal Biochem.* **351**, 44-49
- 29 Douglas, P., Kriek, M., Bryant, P. and Roach, P. L. (2006) Lipoyl synthase inserts sulfur atoms into an octanoyl substrate in a stepwise manner. *Angew Chem Int Ed Engl.* **45**, 5197-5199
- 30 Lanz, N. D., Pandelia, M. E., Kakar, E. S., Lee, K. H., Krebs, C. and Booker, S. J. (2014) Evidence for a Catalytically and Kinetically Competent Enzyme-Substrate Cross-linked Intermediate in Catalysis by Lipoyl Synthase. *Biochemistry*
- 31 Adams, P. D., Afonine, P. V., Bunkoczi, G., Chen, V. B., Davis, I. W., Echols, N., Headd, J. J., Hung, L. W., Kapral, G. J., Grosse-Kunstleve, R. W., McCoy, A. J., Moriarty, N. W., Oeffner, R., Read, R. J., Richardson, D. C., Richardson, J. S., Terwilliger, T. C. and

- Zwart, P. H. (2010) PHENIX: a comprehensive Python-based system for macromolecular structure solution. *Acta Crystallogr D Biol Crystallogr.* **66**, 213-221
- 32 Emsley, P. and Cowtan, K. (2004) Coot: model-building tools for molecular graphics. *Acta Crystallogr D Biol Crystallogr.* **60**, 2126-2132
- 33 Labute, P. (2009) Protonate3D: assignment of ionization states and hydrogen coordinates to macromolecular structures. *Proteins.* **75**, 187-205
- 34 (2013) Molecular Operating Environment, 2013.08. ed.)^eds.), Chemical Computing Group Inc., 1010 Sherbooke St. West, Suite #910, Montreal, QC, Canada, H3A 2R7
- 35 Halgren, T. A. (1996) Merck molecular force field .1. Basis, form, scope, parameterization, and performance of MMFF94. *Journal of computational chemistry.* **17**, 490-519
- 36 Morris, G. M., Huey, R., Lindstrom, W., Sanner, M. F., Belew, R. K., Goodsell, D. S. and Olson, A. J. (2009) AutoDock4 and AutoDockTools4: Automated docking with selective receptor flexibility. *Journal of computational chemistry.* **30**, 2785-2791
- 37 Ho, B. K. and Gruswitz, F. (2008) HOLLOW: generating accurate representations of channel and interior surfaces in molecular structures. *BMC structural biology.* **8**, 49
- 38 Kriek, M., Peters, L., Takahashi, Y. and Roach, P. L. (2003) Effect of iron-sulfur cluster assembly proteins on the expression of Escherichia coli lipoic acid synthase. *Protein Expr Purif.* **28**, 241-245
- 39 Dowling, D. P., Vey, J. L., Croft, A. K. and Drennan, C. L. (2012) Structural diversity in the AdoMet radical enzyme superfamily. *Biochim Biophys Acta.* **1824**, 1178-1195
- 40 Vey, J. L. and Drennan, C. L. (2011) Structural insights into radical generation by the radical SAM superfamily. *Chem Rev.* **111**, 2487-2506
- 41 Holm, L. and Rosenstrom, P. (2010) Dali server: conservation mapping in 3D. *Nucleic Acids Res.* **38**, W545-549
- 42 Nicolet, Y., Rubach, J. K., Posewitz, M. C., Amara, P., Mathevon, C., Atta, M., Fontecave, M. and Fontecilla-Camps, J. C. (2008) X-ray structure of the [FeFe]-hydrogenase maturase HydE from *Thermotoga maritima*. *J Biol Chem.* **283**, 18861-18872
- 43 Vey, J. L., Yang, J., Li, M., Broderick, W. E., Broderick, J. B. and Drennan, C. L. (2008) Structural basis for glycy radical formation by pyruvate formate-lyase activating enzyme. *Proc Natl Acad Sci U S A.* **105**, 16137-16141
- 44 Dowling, D. P., Croft, A. K. and Drennan, C. L. (2012) Radical use of Rossmann and TIM barrel architectures for controlling coenzyme B12 chemistry. *Annual review of biophysics.* **41**, 403-427
- 45 Mao, L., Wang, Y., Liu, Y. and Hu, X. (2003) Multiple intermolecular interaction modes of positively charged residues with adenine in ATP-binding proteins. *J Am Chem Soc.* **125**, 14216-14217
- 46 McIver, L., Baxter, R. L. and Campopiano, D. J. (2000) Identification of the [Fe-S] cluster-binding residues of Escherichia coli biotin synthase. *J Biol Chem.* **275**, 13888-13894
- 47 Mansy, S. S., Xiong, Y., Hemann, C., Hille, R., Sundaralingam, M. and Cowan, J. A. (2002) Crystal structure and stability studies of C77S HiPIP: a serine ligated [4Fe-4S] cluster. *Biochemistry.* **41**, 1195-1201
- 48 Nicolet, Y., Martin, L., Tron, C. and Fontecilla-Camps, J. C. (2010) A glycy radical as the precursor in the synthesis of carbon monoxide and cyanide by the [FeFe]-hydrogenase maturase HydG. *FEBS Lett.* **584**, 4197-4202
- 49 Roy, A., Solodovnikova, N., Nicholson, T., Antholine, W. and Walden, W. E. (2003) A novel eukaryotic factor for cytosolic Fe-S cluster assembly. *EMBO J.* **22**, 4826-4835
- 50 Forzi, L., Koch, J., Guss, A. M., Radosevich, C. G., Metcalf, W. W. and Hedderich, R. (2005) Assignment of the [4Fe-4S] clusters of Ech hydrogenase from *Methanosarcina barkeri*

to individual subunits via the characterization of site-directed mutants. *FEBS J.* **272**, 4741-4753

51 Kato, S., Mihara, H., Kurihara, T., Takahashi, Y., Tokumoto, U., Yoshimura, T. and Esaki, N. (2002) Cys-328 of IscS and Cys-63 of IscU are the sites of disulfide bridge formation in a covalently bound IscS/IscU complex: implications for the mechanism of iron-sulfur cluster assembly. *Proc Natl Acad Sci U S A.* **99**, 5948-5952

52 Miller, J. R., Busby, R. W., Jordan, S. W., Cheek, J., Henshaw, T. F., Ashley, G. W., Broderick, J. B., Cronan, J. E., Jr. and Marletta, M. A. (2000) Escherichia coli LipA is a lipoyl synthase: in vitro biosynthesis of lipoylated pyruvate dehydrogenase complex from octanoyl-acyl carrier protein. *Biochemistry.* **39**, 15166-15178

53 Challand, M. R., Ziegert, T., Douglas, P., Wood, R. J., Kriek, M., Shaw, N. M. and Roach, P. L. (2009) Product inhibition in the radical S-adenosylmethionine family. *FEBS Lett.* **583**, 1358-1362

54 Broderick, J. B., Duffus, B. R., Duschene, K. S. and Shepard, E. M. (2014) Radical S-adenosylmethionine enzymes. *Chem Rev.* **114**, 4229-4317

55 Ugulava, N. B., Gibney, B. R. and Jarrett, J. T. (2001) Biotin synthase contains two distinct iron-sulfur cluster binding sites: chemical and spectroelectrochemical analysis of iron-sulfur cluster interconversions. *Biochemistry.* **40**, 8343-8351

56 Jameson, G. N., Cosper, M. M., Hernandez, H. L., Johnson, M. K. and Huynh, B. H. (2004) Role of the [2Fe-2S] cluster in recombinant Escherichia coli biotin synthase. *Biochemistry.* **43**, 2022-2031

57 Choi-Rhee, E. and Cronan, J. E. (2005) Biotin synthase is catalytic in vivo, but catalysis engenders destruction of the protein. *Chem Biol.* **12**, 461-468

58 Tse Sum Bui, B., Mattioli, T. A., Florentin, D., Bolbach, G. and Marquet, A. (2006) Escherichia coli biotin synthase produces selenobiotin. Further evidence of the involvement of the [2Fe-2S]₂⁺ cluster in the sulfur insertion step. *Biochemistry.* **45**, 3824-3834

59 Farrar, C. E., Siu, K. K., Howell, P. L. and Jarrett, J. T. (2010) Biotin synthase exhibits burst kinetics and multiple turnovers in the absence of inhibition by products and product-related biomolecules. *Biochemistry.* **49**, 9985-9996

Figure Legends.

Figure 1 Biosynthesis of lipoyl cofactors

Figure 2 Overall fold and structure of *TeLipA2*

Residues in all panels are colored as follows: N-terminal extension, pink; RS ($\beta\alpha$)₆ ³/₄ TIM barrel core, green; C-terminal extension, blue. (A) *TeLipA2* complexed with DTT (white) and MTA (yellow). (B) *TeLipA2* complexed with SAH (pale pink). (C) Topology of *TeLipA2*.

Figure 3 *TeLipA2* active site interactions

(A) *TeLipA2* complexed with MTA (yellow) and DTT (pink) with a 2Fo-Fc electron density map contoured at 1 σ . (B) *TeLipA2* complexed with SAH and showing the sodium ion. The 2Fo-Fc electron density map contoured at 1 σ surrounds these ligands and the radical SAM (RS) and auxiliary (Aux) clusters. (C). *TeLipA2*:MTA interactions with MTA and DTT. Functionally conserved motifs identified from other radical SAM enzymes include the CXXXXCX ϕ C motif (in purple, residues 63-70), the 'GGE' motif (blue, residues 105-107), the 'ribose' motif (cyan, residues 167-170), the 'GxIGxxE' motif (pink, residues 208-215) and the β 6 motif (orange, residues 238-241)[39, 40].

Figure 4. Model of *TeLipA2* complexed with SAM and an octanoyl substrate

In all panels the SAM is colored yellow and the octanoyl substrate is colored cyan. (A). Overall view showing the octanoyl channel (cyan surface) and the C-channel (pink surface). The channel surfaces were prepared with HOLLOW [37]. (B). Space filling model showing van der Waals surfaces. Residues 25-29 and 51 to 55 have been omitted for clarity. (C). Distances between reaction centers. (D). The C-channel, showing access to the auxiliary cluster.

Figure 5 Activity assays of serine ligand mutants Ser267Ala and Ser267Cys

Figure 6 Proposed mechanism of lipoyl synthase

Figures and tables

Table 1. Data collection and refinement statistics

	SAD WT LipA:SAH	Native WT LipA:SAH	Native WT LipA:MTA
Data collection			
Wavelength	1.7372	0.9795	0.9795
Space group	C222 ₁	C222 ₁	C222 ₁
Cell dimensions			
<i>a</i> , <i>b</i> , <i>c</i> (Å)	70.52, 161.36, 59.57	71.09, 161.13, 59.47	70.88, 162.80, 58.60
α , β , γ (°)	90.0, 90.0, 90.0	90.0, 90.0, 90.0	90.0, 90.0, 90.0
Resolution (Å)	64.62-2.36	43.89-1.623 (1.691- 1.623)	64.99-1.60 (1.657- 1.600)
<i>R</i> _{sym} or <i>R</i> _{merge}	0.095 (0.508)	0.047 (0.757)	0.037 (0.601)
<i>I</i> / σ <i>I</i>	15.0 (4.5)	16.2 (2.89)	14.96 (2.19)
Completeness (%)	99.8 (99.3)	99.6 (99.1)	97.96 (98.45)
Redundancy	12.7 (12.9)	7.2 (7.1)	4.4 (4.7)
Refinement			
No. reflections		43389 (4260)	44253 (4385)
<i>R</i> _{work}		0.1781 (0.2735)	0.2027 (0.3644)
<i>R</i> _{free}		0.2069 (0.3156)	0.2415 (0.4110)
No. atoms		4529	4356
Protein		2170	2064
Ligands/ions		17	44
Waters		172	181
<i>B</i> -factors			
Protein		36.70	36.80
Ligands/ions		31.60	32.20
Waters		42.2	41.30
R.m.s. deviations			
Bond lengths (Å)		0.014	0.015
Bond angles (°)		2.19	1.960
PDB Code		4U0O	4U0P

Statistics for the highest-resolution shell are shown in parentheses.

Figure 1

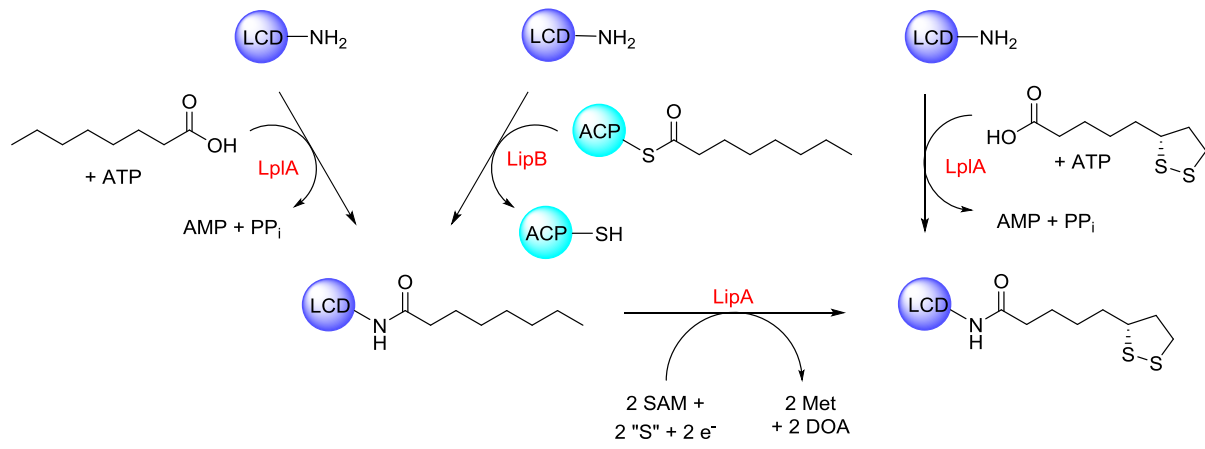


Figure 2

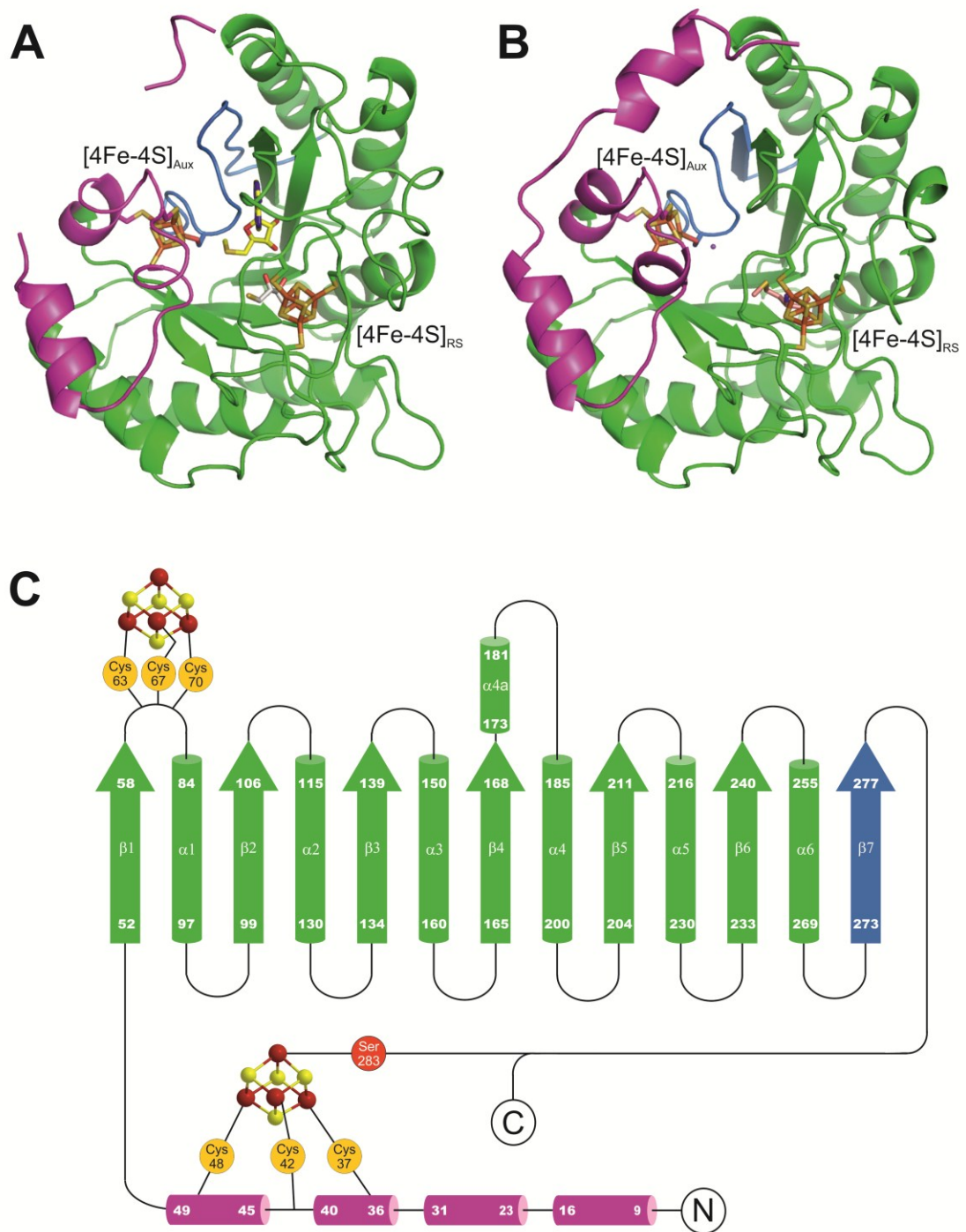


Figure 3

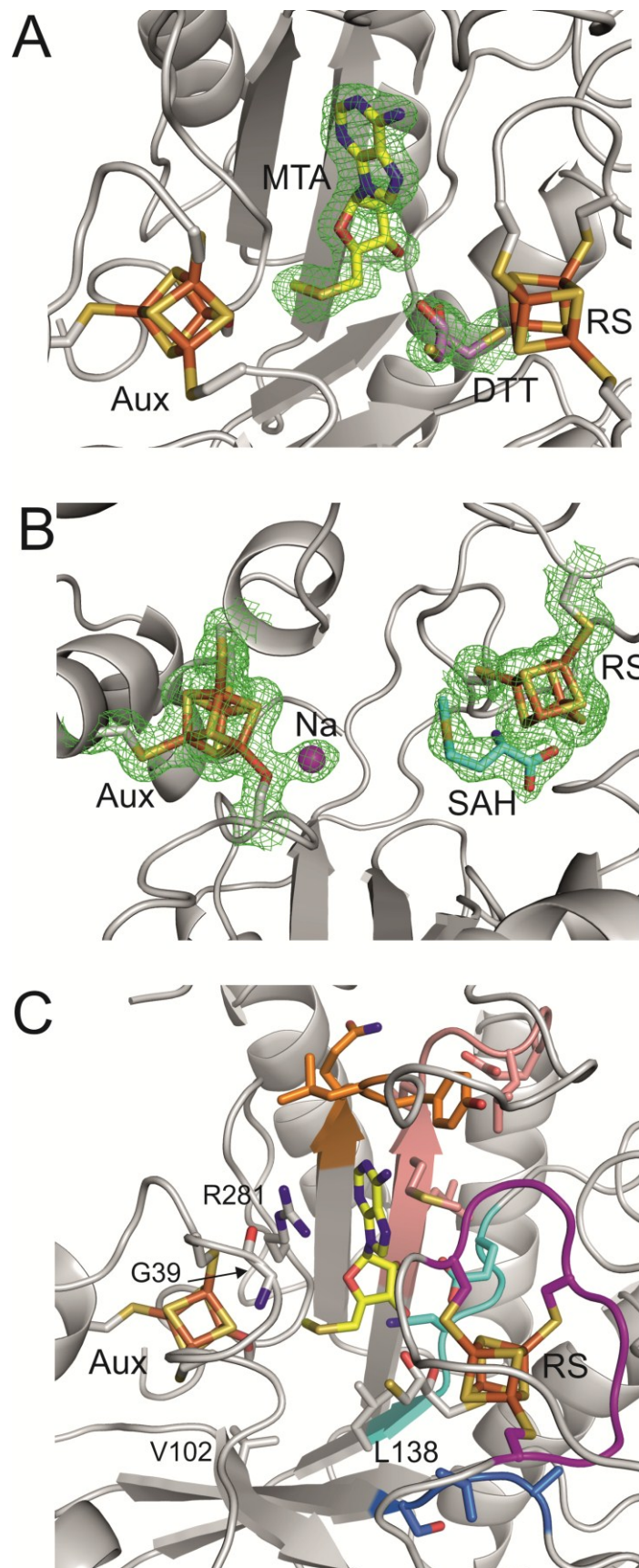


Figure 4

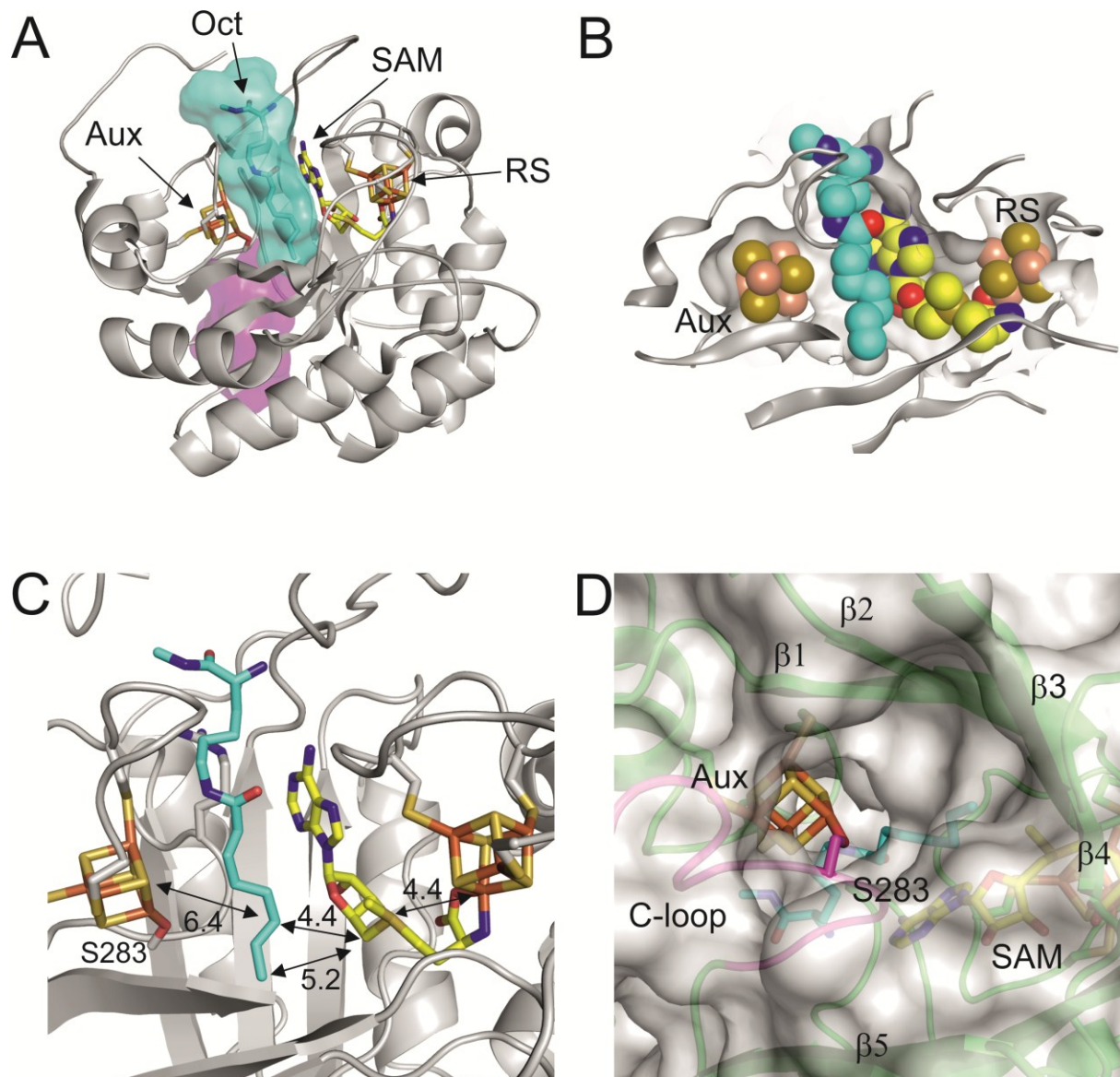


Figure 5

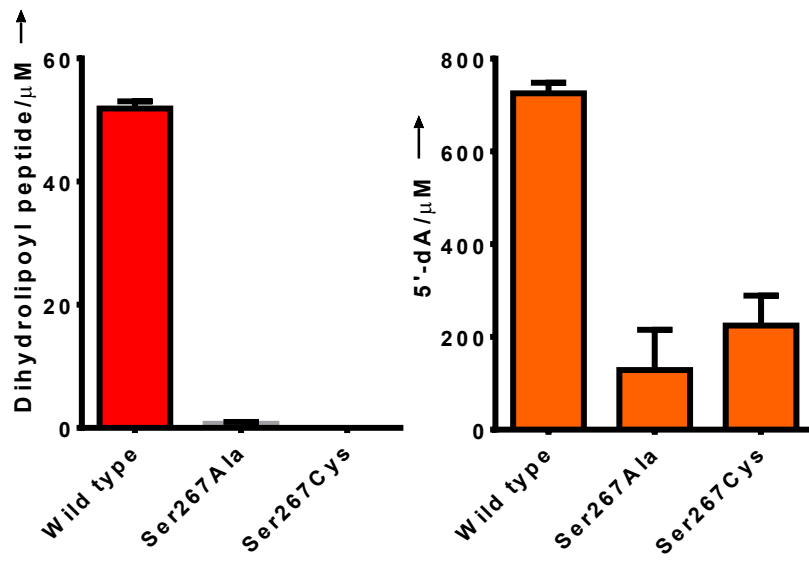


Figure 6

